CHEMISTRY OF MATERIALS

ARTICLE

pubs.acs.org/cm

Hierarchical Zeolite Beta via Nanoparticle Assembly with a Cationic Polymer

Karin Möller,*[,†] Bilge Yilmaz,[‡] Ulrich Müller,[‡] and Thomas Bein*[,†]

[†]Department of Chemistry and Center for NanoScience (CeNS), University of Munich (LMU), Butenandtstrasse 11 (E), D-81377 Munich, Germany

[‡]Chemicals Research & Engineering, BASF SE, Ludwigshafen 67056, Germany

Supporting Information

ABSTRACT: Nanozeolite aggregates with secondary pores of tunable sizes were prepared by the flocculating action of a cationic polymer. Specifically, highly concentrated zeolite beta precursor gels were hydrothermally converted in the presence of the cationic polymer polydiallyldimethylammonium chloride (PDDA). Without polymer, highly crystalline zeolite beta in the form of nanosized particles was obtained from colloidal solutions at high yield. Upon addition of polymer, these nanoparticles were flocculated into self-sustaining, easily retrievable mesoporous aggregates in a one-step procedure at nearly 100% yield, showing interparticle pores with very high mesopore volumes and surface areas. The influence of the amount of polymer, its molecular weight as well as the nature of the silica precursor on pore characteristics, crystallinity, and morphology were studied with nitrogen sorption, mercury intrusion porosimetry and electron microscopy, respectively. Changing the polymer concentration is a powerful parameter to effectively tune the interstitial pore size between 40 and 400 nm by controlling the growth of the zeolite beta particles.

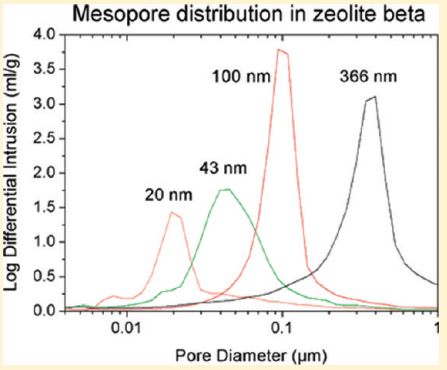

KEYWORDS: hierarchical zeolite beta, nanoparticles, tunable pores, polymer

INTRODUCTION

The quest for optimizing catalytic conversion by facilitating diffusion of reactants and products and controlling coke formation has recently stimulated much research on hierarchical zeolitic materials. Several review articles have appeared on this topic, discussing the different strategies to create additional mesoporosity in these microporous materials.[1−8] In general, a second or even third pore system in form of meso- and/or macropores can be created via either nontemplating or templating synthesis procedures, respectively. The former approach intends to create a secondary pore system through a postsynthesis treatment by steaming[9] or partial leaching of zeolite lattice elements, which is often restricted in pore volume and can also reduce the microporosity.[10−13] On the other hand, templating procedures offer the opportunity to generate a controlled and possibly variable mesopore system, determined by the size and/or amount of the structure-forming additive. "Soft" templating strategies using surfactant molecules as secondary structure-directing agents have often resulted in a composite of amorphous mesoporous silica and zeolitic precursors or crystalline zeolites.[14−17] On the other hand, recrystallization of zeolite Y in the presence of a surfactant resulted in impressively homogeneous mesopores, however accompanied by a loss of about 50% of the micropore volume.[18]

Truly mesoporous spongelike MFI zeolites were obtained by the group of Ryoo when using specifically designed amphiphilic organosilane surfactants as secondary porogens that prevented phase segregation.[19] Silylated polyethyleneimine was used in the group of Pinnavaia as additive in the MFI synthesis and resulted in intracrystalline mesopores.[20] Mesoporous MFI nanoparticle aggregates were also obtained by Serrano et al. by functionalizing zeolite seeds with different organosilanes.[21−23] However, the mesopore size achieved by these procedures was limited to about 2−7 nm. Choi et al. further introduced a new strategy by using novel cyclic diammonium cations bridged by phenyl or diphenyl linkers that stimulated immediate gelation to form a mesoporous gel. The latter was transformed into hierarchical zeolite beta by a pseudomorphic crystallization process resulting in larger mesopores.[24] Recently, this group fabricated truly ordered mesoporous MFI by using linear gemini-type templates consisting of several bridged ammonium cations terminated by long alkyl chains. Changing the bridges from C_6-alkyl- to phenyl groups allowed the synthesis of disordered mesoporous beta nanoparticles with very high surface areas and mesopore volumes.[25]

"Hard" porogens as found in biotemplates, carbon nanotubes or carbon particles that are simply added during zeolite synthesis can be effective for achieving a predetermined pore size.[26−28] Moreover, more elaborate methods using imprints or reverse-templating approaches using preorganized carbon scaffolds have also been reported.[29,30] Here, a systematic variation of the

Received: December 12, 2010
Revised: July 25, 2011
Published: September 16, 2011

mesopore arrangement can be obtained by carefully adjusting the sacrificial templating networks. However, building the architecture of these molds usually requires several reaction steps before even starting the zeolite synthesis.

In the present study, we report on an efficient method for creating mesoporosity in a convenient one-step process that also permits control of the mesopore size and pore volume of hierarchical zeolite beta. Recent publications by the group of Xiao et al. have documented that the synthesis of zeolite beta with the readily available cationic polymer polydiallyldimethylammonium chloride allowed them to introduce mesopore volumina of about 0.17 mL/g.[31,32] Recently, they showed that adding increasing amounts of this polymer caused the formation of larger mesopore volumes of up to 0.41 mL/g as determined from nitrogen sorption and suggested the use of cationic polymers as a general tool for controlling the properties of mesoporous zeolites.[33] Zhu et al. have achieved comparable secondary pore volumes for zeolite beta with the noncharged polyvinyl butyral gel.[34] A further increase in these porosity values was achieved by the group of Xiao when they used a more elaborate two-step approach. Here, a solution of zeolite beta nanoparticles was first prepared by heating the zeolite beta precursor gel at 140 °C for 3 days, followed by adding the polymer to this zeolite slurry. After heating a second time for three days, they obtained a high mesopore volume (0.84 mL/g) for hierarchical zeolite beta with a yield of 66%. The final material consisted of agglomerates of about 150 nm zeolite beta particles separated by smaller, about 20 nm sized crystals, giving rise to a total surface area of about 600 m^2/g.[35] We note that this is the only report where the microporosity of the zeolite phase is almost identical to bulk zeolite beta. Usually, a decrease of microporosity is encountered with increasing mesoporosity.

In the present study we have used a highly concentrated (dense) gel protocol for the synthesis of zeolite beta, intended to stimulate nucleation and to decrease the zeolite domain size.[36] Nanozeolites have been repeatedly suggested to be excellent candidates for enhancing mass transport in catalytic applications due to intrinsically short diffusion paths.[4,6,7] The assembly of nanozeolites into hierarchical materials is usually performed in a multistep approach, where nanozeolites are first produced and subsequently assembled via an additional soft and/or hard scaffold.[37−39] Very few reports exist about the direct assembly of nanozeolites during synthesis. For instance, a three-step temperature treatment is used by Huang et al. to obtain submicrometer NaY aggregates consisting of about 30 nm crystallites.[40] Interestingly, the overall particle size was determined by the water concentration in the dense gel. Previously, Fang et al. assembled nano ZSM-12 particles into submicrometer assemblies via a dense gel synthesis, however, the tuneability of the mesopore size was not shown.[41] Li et al. prepared first silica/alumina nanospheres assisted by the addition of L-lysine, which were then packed by drying and subsequently converted into aggregated nano MFI zeolites via a steam treatment.[42] Holland prepared a highly diluted precursor solution that was first refluxed and then converted into aggregated MFI particles via hydrothermal treatment.[43] A recent report by the group of Larsen[44] describes the preparation of hierarchical beta zeolites from nanoparticles. The nanocrystals are produced in a multiple-step procedure of evaporation, dilution, pH-adjustment, crystallization and subsequent centrifugation that result in mesoporous materials derived from packing of the retrieved nanozeolite powders.

Here we use the cationic polymer polydiallyldimethylammonium chloride (PDDA) as a flocculating agent for in situ formed nanozeolites in order to create hierarchical zeolites by assembling these nanoparticles in one step into stable, easily retrievable (not by centrifugation) aggregates, without additional scaffolds. Tunability of the secondary pores is achieved by changing the polymer concentration.

The reaction was performed with polymers of different molecular weights, ranging from about 100.000 to about 500.000 g/mol. Further, two different silica sources were studied, consisting either of about 50 μm mesoporous silica grains or of colloidal silica. To study the influence of the polymer on mesopore formation, we compare the synthesis performed without polymer addition to results obtained with varying polymer amounts. We demonstrate that by adapting the reaction composition it is possible to obtain large, easily retrievable pieces of mesoporous beta with an adjustable mesopore/macropore size between 40 and about 400 nm.

EXPERIMENTAL SECTION

Sample Preparation. The synthesis was performed with sodium hydroxide (NaOH, 97%), aluminum sulfate ($Al_2(SO_4)_3 \cdot 16H_2O$, Aldrich), tetraethyl ammonium hydroxide (TEAOH, 35% aqueous solution, BASF), mesoporous silica, here named "Si415", (ACROS) 40−60 μm particles with a surface area of 270 m^2/g, 0.01 mL/g μ-pore-volume, and 15 nm pores, or CAB-O-SIL EH-5, 7 nm sized with 0.2−0.3 μm aggregated particle size and 380 m^2/g surface area, and aqueous polydiallyldimethylammonium chloride solutions (PDDA, Aldrich), with molecular weights <100.000 (PDDA-VL, 35 wt %), 100.000−200.000 (PDDA-100, 20 wt %), and 400.000−500.000 (PDDA-400, 20 wt %), respectively.

Standard molar reactant ratios for the dense gel synthesis were (Si/Al ratio = 22):

$$1SiO_2 : 0.023Al_2O_3 : 0.049NaOH : 0.425TEAOH : 6.2H_2O$$

The reactions were carried out as follows:

0.066 g of NaOH, 0.480 g of $Al_2(SO_4)_3 \cdot 16H_2O$, and 6 g of 35% aqueous TEAOH were mixed and stirred until clear (15 to 30 min). The amount of 2.0 g of silica was combined with this solution resulting in a viscous gel, which was further stirred for about 1 h. The desired amount of polymer was added to this gel (listed as g of pure polymer/g SiO_2, from 0.05 to 0.5 g/g) and stirred for ca. 15 min. Highly viscous pastes were obtained at this step, which had to be kneaded in cases where CAB-O-SIL EH-5 was the silica of choice. The gel was subsequently transferred into 20 mL Teflon-lined Parr bombs and heated at 150 °C for 3 days. A reference sample was treated without additional polymer under otherwise similar conditions.

The converted gels were quenched by immersion of the reactor in water at room temperature, retrieved by filtration, washed and dried. Template removal was performed by calcination in air with a temperature profile of 2 °C/min to 550 °C, where it was kept for 6 h.

Characterization. X-ray diffraction data were collected on a STOE powder diffractometer in transmission geometry with Cu−Kα_1 radiation (λ = 1.540 Å). SEM micrographs were obtained on the field emission microscope JEOL JSM-6500F with uncoated powders immobilized on sample holders with silver paste, using 4 keV. Transmission electron microscopy was performed with a JEOL JEM 2011 instrument at 200 kV. Zeolite powder was immersed in ethanol and sonicated for about 30 min, and one to two drops were spread on copper grids covered with holey carbon.

Nitrogen sorption isotherms at −196 °C were measured on previously evacuated samples (at 150 °C overnight) using a Quantachrome Nova 4000e instrument. Micropore volumes were estimated from

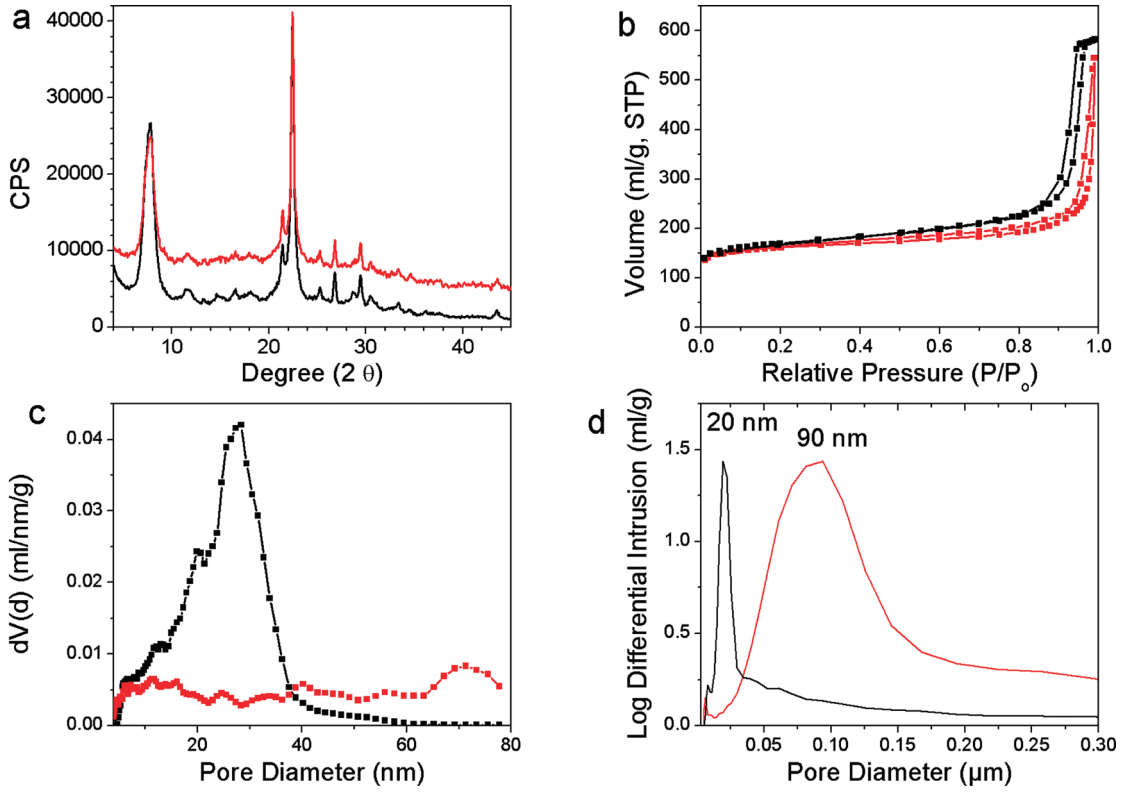

Figure 1. Comparison of zeolite beta obtained from colloidal solution, BSi-0 (black), and from polymer-assisted synthesis, BSiVL-0.1 (red), (a) X-ray diffractograms (red curve is offset by 2000 CPS), (b) nitrogen sorption isotherms, (c) pore-size distributions as derived from nitrogen sorption (NLDFT on the adsorption branch), and (d) from mercury intrusion measurements.

t-plots in the range between 0.12 and 0.5 p/p_0 (de Boer). The apparent surface areas were determined with the Brunauer−Emmett−Teller (BET) model in the range between p/p_0 = 0.03−0.16. The total pore volume was evaluated at p/p_0 = 0.99. Pore size calculations were performed with the DFT method on the adsorption branch using the nitrogen on silica, cylindrical pore NLDFT kernel. Mercury intrusion porosimetry was applied to determine meso- and macropore sizes between 3 nm and 300 μm with a Micromeritics Autopore IV 9520 Mercury Intrusion Porosimeter. Dynamic light scattering (DLS) was measured on a Malvern Zetasizer Nano ZS in aqueous solutions in 1.5 mL PMMA cuvettes. Thermogravimetric measurements were performed on a Netzsch STA 440 C Jupiter TG/DSC instrument with a heating rate of 10 degrees/minute in synthetic air (25 mL/min).

RESULTS AND DISCUSSION

The zeolite beta dense gel synthesis as reported here was always performed at 150 °C for 3 days. In order to study the influence of the secondary structure-directing agent polydiallyldimethylammonium chloride on the mesopore formation, we varied the amount as well as the molecular weight of the polymer during crystallization. Large mesoporous silica grains as well as 200 nm-sized CAB-O-SIL powders were used as Si-precursors, which will be abbreviated as Si or C in the sample names. The amount of g polymer/g silica precursor is added to sample names.

1. Influence of Increasing Concentrations of the Low-Molecular-Weight Polymer PDDA-VL Using Mesoporous Silica As Precursor. In the following we will describe how a systematic increase of polymer amount will affect the physical properties of the hierarchical beta zeolites when the PDDA-VL polymer and the mesoporous silica precursor was used (VL stands for the very low molecular weight polymer; MW <100.000). When the dense-gel synthesis was performed as described in the experimental part without the addition of any polymer, a colloidal solution of zeolite beta was obtained. The grain size of the individual particles of about 40 to 130 nm, as determind with dynamic light scattering (see the Supporting Information), was too small to retrieve the resulting zeolite powder via filtration. Time-consuming high speed centrifugation and washing had to be performed three times to collect a glassy gel. Still, a yield of almost 75% zeolite beta was obtained with this dense gel synthesis, which is very high when compared with the clear-solution synthesis usually applied for nanosized beta.[45−47] In contrast, if a small amount of 0.1 g of PDDA-VL polymer per g precursor silica was administered during the synthesis, flocculation of these nanoparticles was induced and it was easy to filter and wash the resulting white powder with conventional filters, retrieving nearly 100% of the material. Both samples, with and without polymer, are highly crystalline as seen in the X-ray diffractograms in Figure 1a. Differences become obvious when their nitrogen sorption data are compared in Figure 1b. Very high micropore volumes of over 0.2 mL/g (see Table 1) and large surface areas of about 660 m^2/g characterize both samples, but the shape of the isotherm of the colloidal sample is different. We do observe a narrow hysteresis that is well-defined by a closed plateau at highest relative nitrogen pressure. NLDFT calculations on the adsorption branch result in a defined pore-size distribution curve with a maximum at 25 nm (Figure 1 c). However, the nitrogen sorption isotherm of the polymer-derived sample BSiVL-0.1 shows similarly a high sorption in this region,

dx.doi.org/10.1021/cm103533e |*Chem. Mater.* 2011, 23, 4301–4310

Table 1. Composition and Surface Properties of Samples

sample	silica	polymer	polymer (g/g silica)	BET surface area (m^2/g)	μ-pore volume (mL/g)	total pore volume (mL/g)	pore size (N_2 adsorption) (nm)	mesopore volume (Hg-intrusion) (mL/g)[a]	pore size (Hg-intrusion) (nm)	particle size (SEM)(nm)
BSi-0	Si415	none		666	0.227	0.90	27	0.55	19	50−80
BSiVL-0.1	Si415	VL	0.1	670	0.237	0.84		0.89	90	100−150
BSiVL-0.2	Si415	VL	0.2	667	0.222	0.52		0.66	250	250−400
BSiVL-0.3	Si415	VL	0.3	635	0.193	0.65	13	0.82	9.4 + 540	
BSiVL-0.4	Si415	VL	0.4	590	0.138	0.88	12	0.76	8	500−1200 + 25
BSiVL-0.5	Si415	VL	0.5	473	0.086	1.06	13/16	1.16	9.5	
BSi100−0.05	Si415	100	0.05	669	0.238	1.09		1.22	39	
BSi100−0.2	Si415	400	0.2	623	0.194	0.61				300 −500
BSi400−0.05	Si415	400	0.05	687	0.226	0.96		1.14	35	60−120
BSi400−0.2	Si415	400	0.2	621	0.187	0.59				100−400 + 25
BCVL-0.05	Cab	VL	0.05	673	0.233	1.11		0.95	43	50−150
BCVL-0.1	Cab	VL	0.1	681	0.268	0.59		1.16	100	
BCVL-0.2	Cab	VL	0.2	696	0.275	0.49		1.32	366	300−500 +25

[a] Between 0.003 and 1 μm.

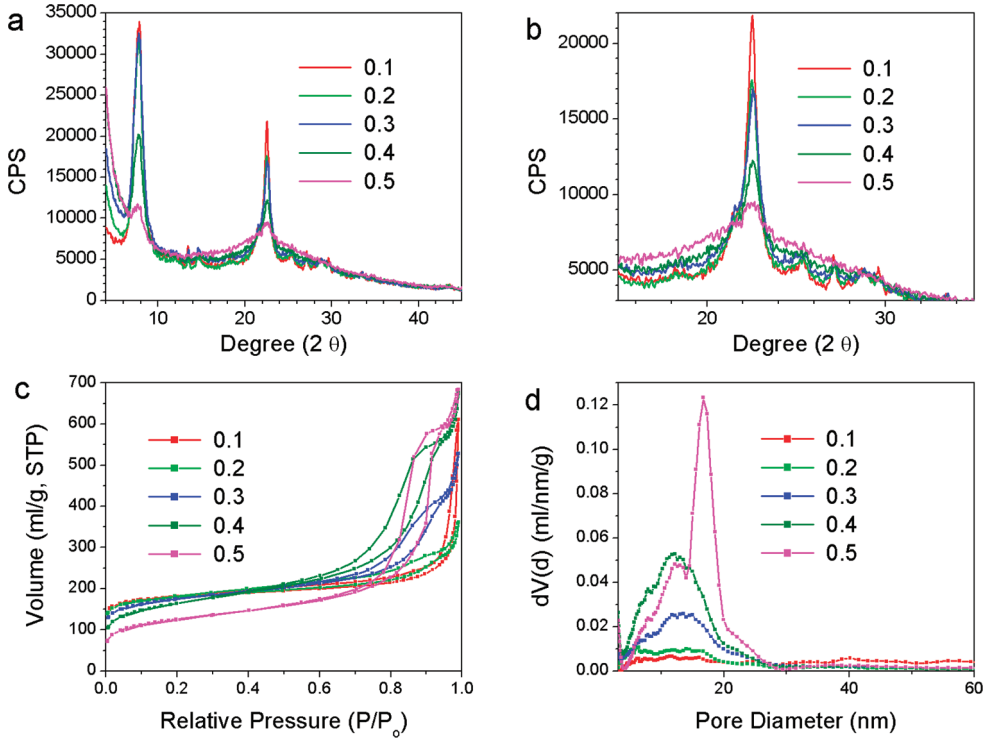

Figure 2. Effect of an increasing amount of very low molecular weight polymer VL on the properties of zeolite beta: (a, b) X-ray diffractograms of calcined samples, b) showing an expanded area of a; (c) nitrogen sorption isotherms, and (d) pore-size distributions from NLDFT calculations of samples: BSiVL-0.1, -0.2, -0.3, -0.4, and -0.5 (same color codes).

but the pore system is not saturated under these conditions and consequently does not allow a pore-size determination from these data. The pore-size evaluation is possible with mercury intrusion porosimetry, which can cover pore sizes between about 3 nm and 300 μm. Figure 1 d compares the pore-sizes of the two samples obtained by the latter method. The powder from the colloidal solution BSi-0 displays a slightly smaller interparticle void size of about 20 nm than the 25 nm evaluated with nitrogen sorption (mercury intrusion pore size evaluation is performed with the BJH method which results in smaller diameters). Additionally, the total mesopore volume of 0.55 mL/g determined from cumulative intrusion for pores between 0.003 to 1 μm is also close to the mesopore volume from nitrogen sorption (total volume − micropore volume, 0.67 mL/g). In sample BSiVL-0.1, however, one can only now detect the complete mesopore/macropore distribution curve, displaying a maximum at about 90 nm. The total mesopore/macropore volume is concomitantly increased to 0.89 mL/g from only

dx.doi.org/10.1021/cm103533e |*Chem. Mater.* 2011, 23, 4301–4310

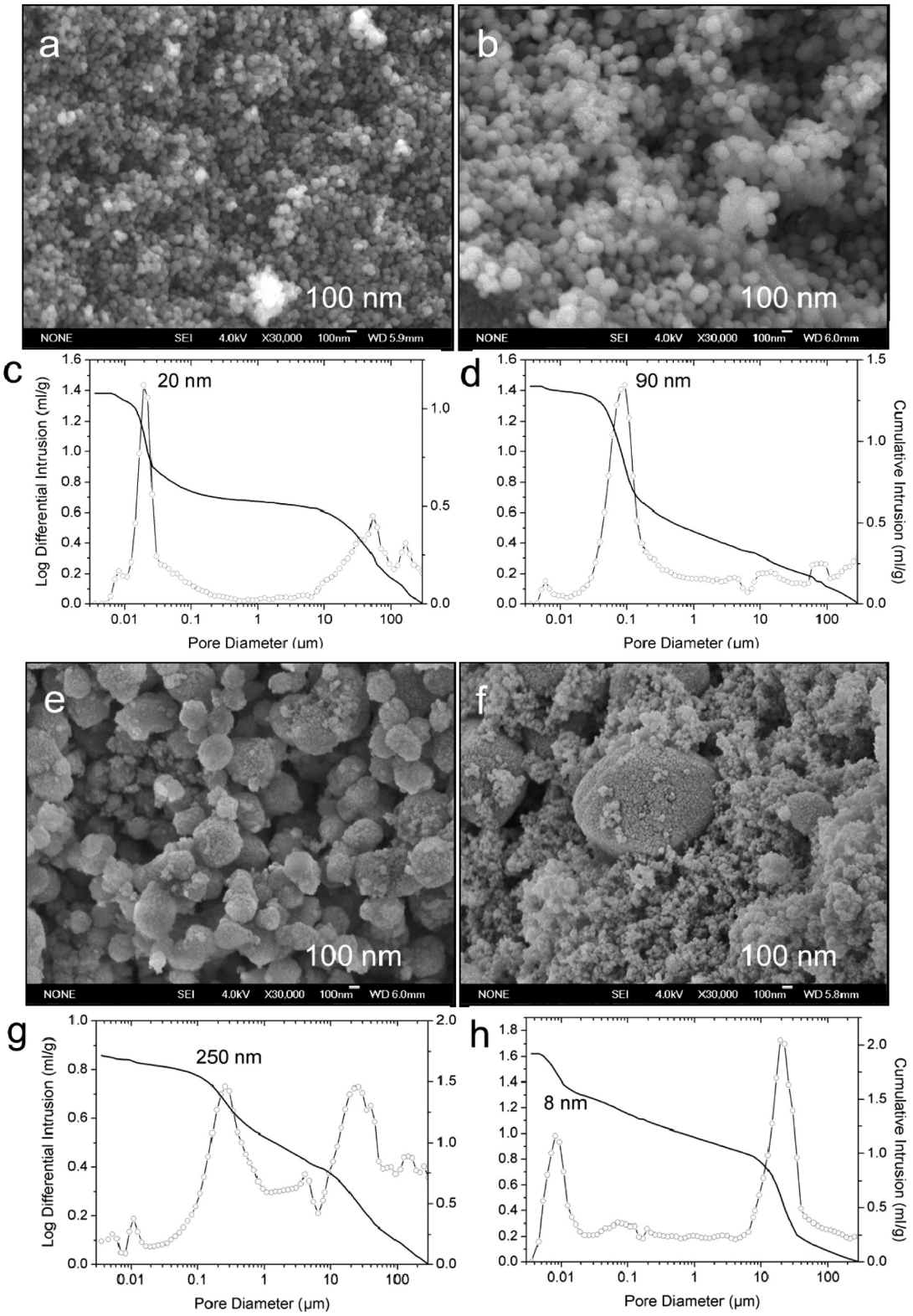

Figure 3. Effect of increasing amount of very low molecular weight polymer VL examined with scanning electron microscopy (all showing the same magnification) and mercury intrusion porosimetry. (a, c) samples BSi-0 without polymer, (b, d) sample BSiVL-0.1, (e, g) sample BSiVL-0.2, and (f, h) sample BSiVL-0.4.

0.6 mL/g determined from nitrogen sorption. The comparison of these samples shows that even small amounts of polymer stimulate a drastically different behavior during zeolite synthesis, resulting in larger, easily retrievable particles, which give rise to larger secondary pores in the final material.

dx.doi.org/10.1021/cm103533e |*Chem. Mater.* 2011, 23, 4301–4310

We ask if this effect can lead to a trend of increasing pore size when the polymer addition is adequately varied. To answer this question, we have successively increased the polymer content from 0.1 to 0.5 g in samples BSiVL-0.1 to BSVL-0.5. Figure 2a displays an overview over diffractograms obtained from these samples after calcination. They are color-coded and overlaid in order to allow the immediate recognition of the reduction in X-ray intensity with increasing amount of polymer content. The concomitant line-broadening and growth of background is amplified in Figure 2b where the region around the [300] and [302] reflections is expanded. Diffractograms of zeolite beta are naturally less defined when compared to other highly crystalline zeolites because of its polymorphic nature. An additional line-broadening could occur when nanoscale crystalline domains would prevail in the powder. Provided the latter feature applies here, it would point to a reduction of zeolite beta crystal sizes scaling with the increasing polymer content in the synthesis mixture. However, if we analyze the corresponding nitrogen sorption isotherms in Figure 2c we observe two major trends: first, we note that the absorption in the low pressure region decreases as soon as the polymer content exceeds 0.2 g/g of SiO_2 (see Table 1). The data show a dramatic trend to smaller values, starting from 0.237 in sample BSiVL-0.1 with low polymer content to only 0.086 mL/g with 0.5 g of polymer/g of SiO_2 in sample BSiVl-0.5. The latter value is too small to account for a fully crystalline sample of nano particles. Even the small colloidal crystallites of sample BSi-0 have a micropore volume of 0.227 mL/g. Simultaneously, we observe a similar trend for the total surface areas as determined by BET analysis, which show decreasing surface areas from 670 to 473 m^2/g with larger polymer content. In contrast, small individual particles should show an increase in surface area with decreasing size. In combination, these data reflect a loss of crystallinity and the presence of a growing amount of nonporous silica when the polymer amounts exceed 0.3 g/g SiO_2. Taking into account the loss in X-ray-intensity, we attribute the apparent line-broadening to an increasing background from unconverted amorphous silica. The large polymer amounts seem to prevent the complete conversion of the amorphous gel quite effectively, because even an extended reaction time of 6 days caused no recognizable change in X-ray crystallinity and sorption data.

A second major trend can be observed in the nitrogen sorption data when the region of higher partial pressure is analyzed. With increasing polymer content, we notice an increase in hysteresis between the adsorption and desorption branch, indicative of the presence of mesopores. The sample with the lowest polymer addition (BSiVL-0.1, red) shows a steep hysteresis starting at the highest partial pressure of all polymer samples. The hysteresis then shifts to lower partial pressures and is growing with larger polymer amount, thus indicating an increase in mesopore volume from sample BSiVL-0.2 (green) to BSiVL-0.5 (purple) (see Table 1). The corresponding pore size distributions are collected in Figure 2d. As mentioned above, the mesopore diameters in the highly crystalline samples BSiVL-0.1 as well as BSiVL-0.2 can not be determined by nitrogen sorption since the pore filling is not completed at the equilibrium pressure of nitrogen. However, the isotherms of samples BSiVL-0.3 to BSiVL-0.5 all show a closed hysteresis. These samples have similar mesopores of about 13 nm diameter with an increase in pore volume.

We thus conclude from the nitrogen sorption data that the mesopore volume of the 13 nm pores is increasing with increasing polymer amount but that this effect is obtained only by incrementally sacrificing some crystallinity in these samples. It should be stressed, however, that the micro- and mesopore volumes as well as surface areas obtained with polymer amounts of up to 0.3 g of polymer/g of silica are high when compared to data in the literature. Micropore values of 0.237 mL/g and concomitant surface areas of 670 m^2/g have rarely been reached; micropore volumes are usually far smaller than 0.2 mL/g and surface areas rarely exceed 600 m^2/g in mesoporous zeolite beta[32,35,48] or even in pure beta nanozeolites made from clear solutions.[46] Thus, a marked loss in crystallinity in our samples is observed only when adding 0.4 g polymer/g SiO_2 or more.

The influence of the polymer content is further reflected in a change of morphology in these samples. Scanning electron microscopy was performed with the colloidal powder BSi-0 as well as samples BSiVL-0.1, BSiVL-0.2 and BSiVL-0.4. Micrographs, all taken at the same magnification, are shown in Figure 3 in combination with mercury intrusion results of the respective samples. The powder BSi-0 that was retrieved from colloidal solution when no polymer was added in the synthesis shows a homogeneous particle size between 50 and 80 nm. The corresponding pore size from mercury intrusion measurements is narrowly distributed around 20 nm (Figure 3a,c). As mentioned earlier, even when only small amounts of polymer were added, we observed flocculation of these nanosized particles into large, self-sustaining aggregates that were easily retrieved by filtration. These aggregates were usually far larger than 10 μm, and had to be lightly crushed for SEM analysis (see also the Supporting Information). The micrometer-sized shards show a systematic change in their composition: the smallest amount of polymer shown here, (BSiVL-0.1, 0.1 g/g SiO_2), causes the aggregation into slightly larger primary particles of about 100−150 nm. This increase in particle size is accompanied by the above-mentioned increase in mesopore size from 20 to 90 nm, the latter showing a significant broadening in the distribution (Figure 3b,d). This growth continues upon further increasing the polymer content in sample BSiVL-0.2, which is composed of particles with 250−400 nm diameter that now generate macropores with sizes around 250 nm (Figure 3e,g). A second peak in the pore size distribution of about 23 μm, as detected in many diagrams, is most likely caused by the macroscopic slabs of the aggregated particles, which are of arbitrary size in each sample. An obvious phase change is visible with even larger polymer content of 0.4 g/g of silica in sample BSiVL-0.4. Here, we observe the formation of a bimodal phase. Some areas in this sample seem to consist of dense films composed of particles with diameters of 25 nm and smaller (see the Supporting Information). In addition, very large particles of about 1 μm or more are visible in other areas (Figure 3f). The interparticle voids between these large assemblies are filled with small nanoparticles.

The bimodal phase causes an immediate drop from macropores to small mesopores with a diameter of only 8 nm when measured with mercury intrusion. This is close to the pore diameter of about 12 nm as derived from nitrogen sorption. Mesopores of similar dimension are also found in sample BSiVL-0.5 where the two methods detect 13 nm (nitrogen sorption) and 9.5 nm pores (mercury intrusion, not shown). Following this development, it is evident that the meso/macropore size originates from interparticle voids and that it is mainly determined by the overall size of the constituting particles in the sample. The respective mesopore volume as determined from Hg-porosimetry is more than 1 mL/g in sample BSiVL-0.5, which is comparable to the mesopore volume derived from nitrogen sorption.

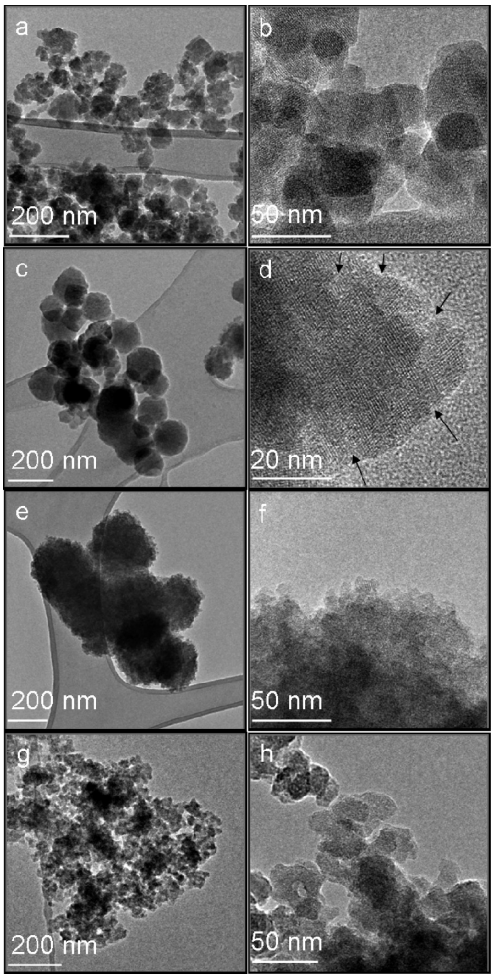

Figure 4. Transmission electron micrographs of samples (a, b) BSi-0 (no polymer), (c, d) BSiVL-0.1 (0.1 g PDDA/g SiO_2), (e, f) BSiVL-0.2 (0.2 PDDA/g SiO_2), and (g, h) BSiVL- 0.3 (0.3 g PDDA/g SiO_2).

Thus both methods detect a steady increase in mesopore volume when polymer amounts are compared from 0.3 to 0.5 (see Table 1). We attribute this increased pore volume to the appearance of a second population of smaller particles due to the increased polymer content.

The differences in sample morphology are best understood with transmission electron microscopy. A comparison of the samples BSi-0, BSiVL-0.1, BSiVL-0.2, and BSiVL-0.3 in Figure 4 shows an apparent increase in global particle sizes. The colloidal sample obtained without polymer consists of small polycrystalline aggregates of 70−100 nm with individual crystals being between 40 and 50 nm in size (Figure 4a). Lattice fringes running throughout each particle in only one direction document the single crystal habit as well as the small size of the particles, which are all transparent to the electron beam (Figure 4b). The addition of small amounts of polymer causes a condensation into larger particles of about 100−150 nm in sample BSiVL-0.1 (Figure 4c). Density differences within the individual particle as seen in Figure 4d are caused by thickness variations (indicated by arrows). This may point to a crystal growth by condensation from very small, otherwise unstable nanoparticles. The resulting rugged particle surface has been observed frequently in nano beta crystallites.[44] In-depth studies of the formation mechanism of zeolite beta by Hould et al. support a growth mechanism through cluster aggregation.[49] Similar suggestions have also been made by Fang et al. for the crystal growth of mesoporous ZSM-12.[41] They used a dense gel synthesis with comparable SiO_2 to H_2O ratios as used in our approach for zeolite beta and obtained morphologically very similar aggregated zeolite particles.

In sample BSiVL-0.2, we observed aggregation to even larger particles of about 100−400 nm (Figure 4e). The habit of these samples has changed again which is visible upon larger magnification. Now, extremely small crystalline domains of about 10 nm appear to be packed into a dense assembly. Because this sample shows high crystallinity in X-ray-diffraction, it must be dominated by crystalline areas that are too thick for evaluation by TEM. Additional polymer dosing in sample BSiVL-0.3 creates numerous loose assemblies of 20−40 nm amorphous gel particles. These did not show any crystallinity in electron diffraction and constitute the 25 nm phase that was observed earlier in the SEM micrographs in samples with large polymer content. Only a few spherical aggregates similar to those in Figure 4e are detected in this sample showing single crystal habit with large, 100 nm-sized areas of continuous lattice fringes (see the Supporting Information).

2. Influence of the Molecular Weight of the Cationic Polymer PDDA. Different molecular weights of the same polymer PDDA were used for the synthesis of zeolite beta. In the following, we document the influence of the 100.000 and 400.000 MW polymer when applied in very small quantities (0.05 g/g SiO_2) and medium quantities (0.2 g/g SiO_2), using again the mesoporous silica precursor. We should note that the samples BSi400-0.05 and BSi100-0.05 could still be retrieved by filtration after completed conversion, even when using the small polymer concentration of 0.05 g/g SiO_2. As shown in Figure 5a, there is no indication for a change in the X-ray crystallinity when polymers with these different molecular weights are used. Similarly, we do not find major differences between the respective nitrogen sorption isotherms (Figure 5b). In these samples the mesopore adsorption occurs again at high relative pressures, comparable to the behavior of sample BSiVL-0.1 in Figure 1b. The pore size distribution was therefore determined with mercury intrusion measurements as shown in Figure 5c. Both samples have nearly identical secondary pores and offer strikingly large mesopore volumes of over 1 mL/g. We note that the pore size of about 39 nm is smaller than the 90 nm obtained with the larger amount of 0.1 g/g SiO_2 in sample BSiVL-0.1, but larger than the 20 nm pores obtained from the colloidal powder. The reason can be found in the particle size by consulting SEM analysis (see the Supporting Information Figure S-5). The sample BSi400-0.05 has a grain size of about 60−120 nm, which lies between the 50−80 nm particles of sample BSi-0 and the 100−150 nm particles in sample BSiVL-0.1, thus resulting in assemblies with intermediate interparticle spaces (see Table 1).

Moreover, no major difference is observed in the nitrogen sorption isotherms when the low-molecular-weight polymer PDDA-100 or polymer PDDA-400 is added in larger quantities of 0.2 g/g of SiO_2 (Figure 6a). Compared to the isotherms with smaller polymer amounts in Figure 5b, we notice a slight influence on the position of the hysteresis toward smaller relative pressure as well as a slight loss in microporosity and surface area. Similar trends were observed with the very low molecular weight polymer VL as described above, thus the effect has to be

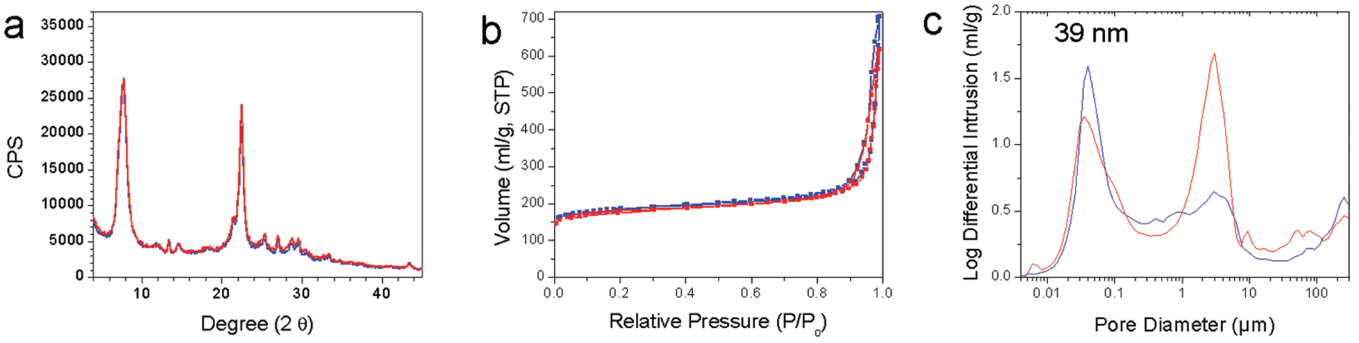

Figure 5. Influence of the polymer molecular weight of polymers PDDA-100 and PDDA-400 on the texture of hierarchical zeolite beta, at 0.05 g/g SiO_2, samples BSi100-0.05 (blue) and BSi400-0.05 (red), (a) XRD of calcined samples, (b) nitrogen sorption isotherms, (c) Hg-intrusion measurements.

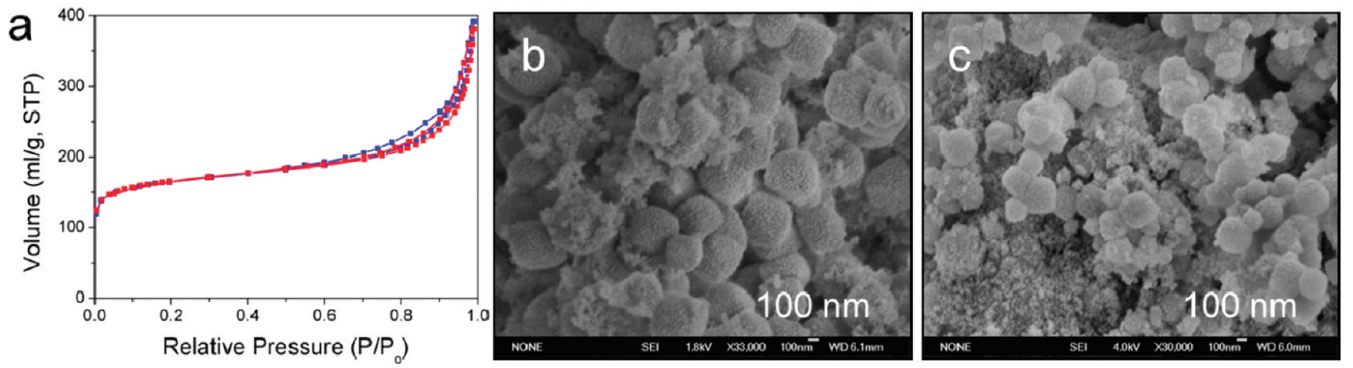

Figure 6. Influence of the polymer molecular weight of polymers PDDA-100 and PDDA-400 on the texture of hierarchical zeolite beta, at 0.2 g/g SiO_2, samples BSi100−0.2 (blue) and BSi400−0.2 (red), (a) nitrogen sorption isotherms, (b, c) scanning electron micrographs.

attributed to the increasing concentration and not to the molecular weight of the polymer. However, if we compare the SEM micrographs of these samples in images b and c in Figure 6 with that of sample BSiVL-0.2 in Figure 3e, we notice a larger amount of very small particles with an increasing molecular weight of the polymer. Thus, the observed phase segregation into different particle sizes appears to start earlier with larger polymers.

3. Effect of the Silica Source. We have further studied the formation of mesoporous zeolite beta under the same reaction conditions by using a different silica source. When we exchanged the 40−60 μm-sized mesoporous silica precursors for a fumed CAB-O-SIL powder we observed very similar trends as discussed above. Nitrogen sorption data show very high surface areas and micropore volumes with polymer contents up to 0.2 g/g silica (see Figure 7a and Table 1). As before, the mesopore size could be adjusted by the amount of polymer, with the least amount of 0.05 g of polymer/g of CAB-O-SIL resulting in the smallest mesopore diameters of about 43 nm (see Figure 7b). The addition of 0.1 g/g polymer increased the peak pore diameter to 100 nm, and 0.2 g/g of polymer to about 370 nm, respectively. These pore sizes are larger than those obtained with the mesoporous silica precursor. For comparison, we also include sample BSi-0 in Figure 7b. SEM analysis shows once more that the above pore sizes are determined by the individual particle sizes, which strongly increased from about 50−150 nm in sample BCVL-0.05 to about 300−500 nm in sample BCVL-0.2, the latter pores being markedly larger than the 100−400 nm pores of sample BSiVL-0.2 (Figure 3g). The size separation into very small and large particles can already be recognized in this sample, thus starting earlier as with the mesoporous silica precursor.

Both sets of experiments with different silica precursors show that the amount of polymer present during the synthesis is a convenient parameter to tune the size of the secondary pores. The smallest mesopore size accessible in the polymer synthesis is about 40 nm before entering the regime of colloidal zeolites, which require time-consuming cleanup procedures. Secondary pores can be obtained up to a size of about 400 nm without degrading the zeolitic characteristics. The pore size is, as we have shown, predominantly determined by the interparticle voids that grow concomitantly to the size of the individual zeolite crystals, and it is not caused by intraparticle voids formed by mesoscale templating with the polymer. The positively charged polymer seems to cause a different flocculation behavior of the negatively charged silica particles depending on polymer concentration. Small amounts of polymer are sufficient to stimulate the aggregation of nanoscale single zeolite crystals into larger particles, which subsequently condense into grains with relatively small mesopores. Beyond a certain polymer concentration, the polymer appears to flocculate the gel components at earlier stages of crystallization, thus finally resulting in mixtures containing large fractions of amorphous gels. Based on these findings, the application of PDDA as porosity-inducing agent for zeolite beta is only effective up to about 0.2 g/g silica, which is efficient for spanning a large range of mesopores/macropores from about 40 to 400 nm.

Recently, we have demonstrated that the mesopore size can further be reduced below 40 nm while still obtaining large

dx.doi.org/10.1021/cm103533e |*Chem. Mater.* 2011, 23, 4301–4310

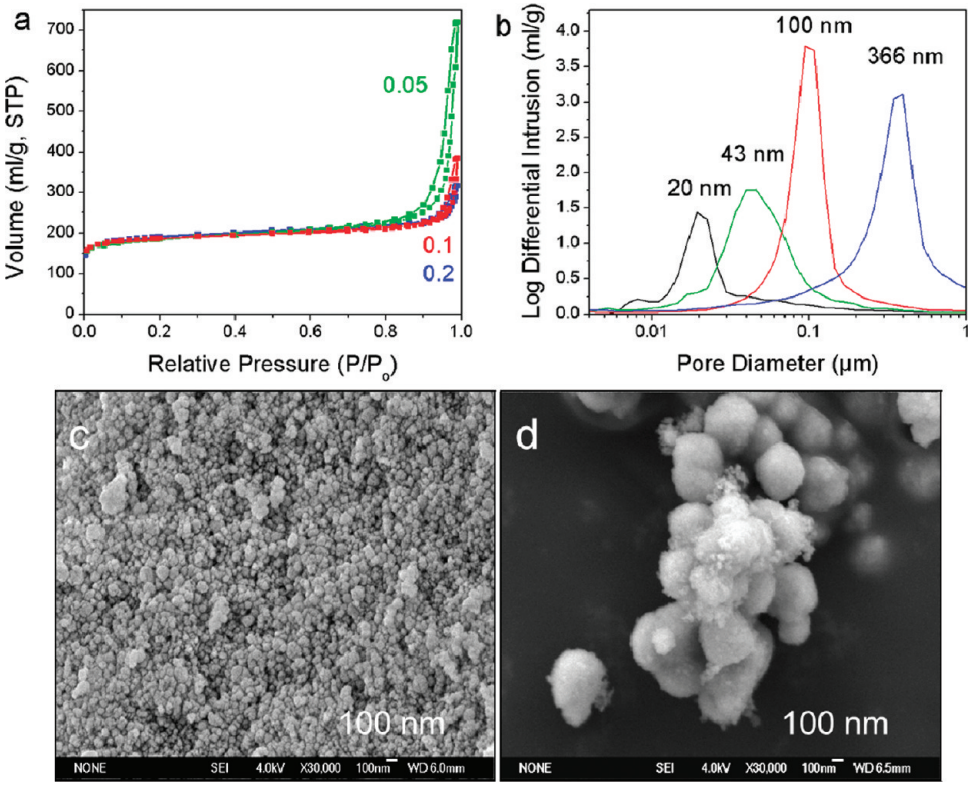

Figure 7. (a) Nitrogen sorption isotherms of samples prepared from CAB-O-SIL with increasing amount of low molecular weight PDDA-VL, sample BCVL-0.05 (green), BCVL-0.1 (red), and BCVL-0.2 (blue), (b) Hg-intrusion porosimetry of samples in a, including sample BSi-0 without polymer (black), (c, d) SEM micrographs of (c) sample BCVL-0.05, (d) sample BCVL-0.2 (at the same magnification).

self-supporting zeolite beta pieces.[50] In this case, self-sustaining nanozeolite aggregates are formed from the same dense gel after drying and applying a steam-assisted conversion without additional porogen. Pores of about 13 nm resulted from interstitial spaces of condensed 20 nm zeolite beta particles. Both approaches have in common that the pore dimensions are determined by the size of the primary crystals. Together, these two strategies offer convenient single-step pathways to fine-tune the pore dimensions of hierarchical zeolite beta to the specific needs of their respective applications.

CONCLUSIONS

In this study, we have evaluated a polymer-based synthetic approach in order to find reaction conditions that result in easily prepared hierarchical zeolite beta materials with tunable mesoporosity. Hydrothermal synthesis was performed with dense gels derived from different silica precursors under addition of varying amounts of PDDA polymer. It was shown that the mesopore/macropore size can be adjusted between about 40 and 400 nm upon increasing the amount of polymer in the synthesis gel, the largest size being obtained with CAB-O-SIL as silica source. Larger amounts of added polymer can result in the reduction of zeolite crystallinity. We have demonstrated that the mesopore size is controlled by the size of primary particles in zeolite beta aggregates, which is strongly influenced by the amount of polymer added. This one-step procedure offers a convenient and inexpensive synthesis route to prepare customized hierarchical zeolitic beta materials within only 3 days of reaction. The hydrothermal conversion of highly concentrated gels provides reaction conditions to generate aggregates of ultrasmall zeolite particles that completely retain their microporosity while simultaneously showing extremely large mesopore volumes of over 0.8 mL/g. Small amounts of added polymer are sufficient to flocculate nanosized beta particles into larger aggregates that permit efficient processing while still offering the favorable features of nanozeolites. We envision that reactant and product diffusion as well as catalytic conversions will benefit substantially from the hierarchical channel systems of these nanomaterials.

ASSOCIATED CONTENT

Supporting Information. SEM, TEM micrographs, X-ray diffractograms, dynamic light scattering, and thermogravimetry. This material is available free of charge via the Internet at http://pubs.acs.org.

AUTHOR INFORMATION

Corresponding Author

*E-mail: bein@lmu.de, Karin.Moeller@cup.uni-muenchen.de. Fax: +49-89-218077622.

ACKNOWLEDGMENT

The authors acknowledge generous funding from BASF SE for this work. We thank Benjamin Mandelmeier for performing the SEM analysis.

REFERENCES

(1) Perez-Pariente, J.; Diaz, I.; Agundez, J. *C. R. Chim.* **2005**, *8*, 569.

(2) Tao, Y.; Kanoh, H.; Abrams, L.; Kaneko, K. *Chem. Rev.* **2006**, *106*, 896.
(3) Meynen, V.; Cool, P.; Vansant, E. F. *Microporous Mesoporous Mater.* **2007**, *104*, 26.
(4) Perez-Ramirez, J.; Christensen, C. H.; Egeblad, K.; Christensen, C. H.; Groen, J. C. *Chem. Soc. Rev.* **2008**, *37*, 2530.
(5) Yang, X.-Y.; Li, Y.; Lemaire, A.; Yu, J.-G.; Su, B.-L. *Pure Appl. Chem.* **2009**, *81*, 2265.
(6) Zhang, Y.; Ren, N.; Tang, Y. *Ordered Porous Solids* **2009**, 441.
(7) Egeblad, K.; Christensen, C. H.; Kustova, M.; Christensen, C. H. *Chem. Mater.* **2008**, *20*, 946.
(8) Chal, R.; Gérardin, C.; Bulut, M.; van Donk, S. *ChemCatChem* **2011**, *3*, 67.
(9) Bernasconi, S.; van Bokhoven, J. A.; Krumeich, F.; Pirngruber, G. D.; Prins, R. *Microporous Mesoporous Mater.* **2003**, *66*, 21.
(10) Caicedo-Realpe, R.; Perez-Ramirez, J. *Microporous Mesoporous Mater.* **2010**, *128*, 91.
(11) Li, X. F.; Prins, R.; van Bokhoven, J. A. *J. Catal.* **2009**, *262*, 257.
(12) Perez-Ramirez, J.; Abello, S.; Bonilla, A.; Groen, J. C. *Adv. Funct. Mater.* **2009**, *19*, 164.
(13) Groen, J. C.; Peffer, L. A. A.; Moulijn, J. A.; Perez-Ramirez, J. *Chem.—Eur. J.* **2005**, *11*, 4983.
(14) Zhao, J.; Hua, Z.; Liu, Z.; Li, Y.; Guo, L.; Bu, W.; Cui, X.; Ruan, M.; Chen, H.; Shi, J. *Chem. Commun.* **2009**, 7578.
(15) Trong-On, D. K.; Kaliaguine, S. *Angew. Chem., Int. Ed.* **2001**, *40*, 3248.
(16) Prokesova, P.; Mintova, S.; Cejka, J.; Bein, T. *Mater. Sci. Eng., C* **2003**, *C23*, 1001.
(17) Gu, F. N.; Wei, F.; Yang, J. Y.; Lin, N.; Lin, W. G.; Wang, Y.; Zhu, J. H. *Chem. Mater.* **2010**, *22*, 2442.
(18) Chal, R.; Cacciaguerra, T.; van Donk, S.; Garardin, C. *Chem. Commun.* **2010**, *46*, 7840.
(19) Choi, M.; Cho Hae, S.; Srivastava, R.; Venkatesan, C.; Choi, D.-H.; Ryoo, R. *Nat. Mater.* **2006**, *5*, 718.
(20) Wang, H.; Pinnavaia, T. J. *Angew. Chem., Int. Ed.* **2006**, *45*, 7603.
(21) Serrano, D. P.; Aguado, J.; Escola, J. M.; Rodriguez, J. M.; Peral, A. *Chem. Mater.* **2006**, *18*, 2462.
(22) Serrano, D. P.; Aguado, J.; Morales, G.; Rodriguez, J. M.; Peral, A.; Thommes, M.; Epping, J. D.; Chmelka, B. F. *Chem. Mater.* **2009**, *21*, 641.
(23) Aguado, J.; Serrano, D. P.; Rodriguez, J. M. *Microporous Mesoporous Mater.* **2008**, *115*, 504.
(24) Choi, M.; Na, K.; Ryoo, R. *Chem. Commun.* **2009**, 2845.
(25) Na, K.; Jo, C.; Kim, J.; Cho, K.; Jung, J.; Seo, Y.; Messinger, R. J.; Chmelka, B. F.; Ryoo, R. *Science* **2011**, *333*, 328–332.
(26) Jacobsen, C. J. H.; Madsen, C.; Houzvicka, J.; Schmidt, I.; Carlsson, A. *J. Am. Chem. Soc.* **2000**, *122*, 7116.
(27) Valtchev, V. P.; Smaihi, M.; Faust, A.-C.; Vidal, L. *Chem. Mater.* **2004**, *16*, 1350.
(28) Schmidt, I.; Boisen, A.; Gustavsson, E.; Sthl, K.; Pehrson, S.; Dahl, S.; Carlsson, A.; Jacobsen, C. J. H. *Chem. Mater.* **2001**, *13*, 4416.
(29) Sakthivel, A.; Huang, S.-J.; Chen, W.-H.; Lan, Z.-H.; Chen, K.-H.; Kim, T.-W.; Ryoo, R.; Chiang, A. S. T.; Liu, S.-B. *Chem. Mater.* **2004**, *16*, 3168.
(30) Egeblad, K.; Kustova, M.; Klitgaard, S. K.; Zhu, K.; Christensen, C. H. *Microporous Mesoporous Mater.* **2007**, *101*, 214.
(31) Xiao, F.-S.; Wang, L.; Yin, C.; Lin, K.; Di, Y.; Li, J.; Xu, R.; Su, D. S.; Schlogl, R.; Yokoi, T.; Tatsumi, T. *Angew. Chem., Int. Ed.* **2006**, *45*, 3090.
(32) Tang, T.; Yin, C.; Wang, L.; Ji, Y.; Xiao, F.-S. *J. Catal.* **2007**, *249*, 111.
(33) Wang, L.; Zhang, Z.; Yin, C.; Shan, Z.; Xiao, F.-S. *Microporous Mesoporous Mater.* **2010**, *131*, 58.
(34) Zhu, H.; Liu, Z.; Kong, D.; Wang, Y.; Xie, Z. *J. Phys. Chem. C* **2008**, *112*, 17257.
(35) Song, J.; Ren, L.; Yin, C.; Ji, Y.; Wu, Z.; Li, J.; Xiao, F.-S. *J. Phys. Chem. C* **2008**, *112*, 8609.
(36) Ding, L.; Zheng, Y. *Microporous Mesoporous Mater.* **2007**, *103*, 94.
(37) Li, P.; Jin, Y.; Zhao, S.; Li, J.; Wang, D. *Petroleum Science and Technology* **2010**, *28*, 852.
(38) Tan, Q.; Bao, X.; Song, T.; Fan, Y.; Shi, G.; Shen, B.; Liu, C.; Gao, X. *J. Catal.* **2007**, *251*, 69.
(39) Kang, Y.; Shan, W.; Wu, J.; Zhang, Y.; Wang, X.; Yang, W.; Tang, Y. *Chem. Mater.* **2006**, *18*, 1861.
(40) Huang, Y.; Wang, K.; Dong, D.; Li, D.; Hill, M. R.; Hill, A. J.; Wang, H. *Microporous Mesoporous Mater.* **2010**, *127*, 167.
(41) Fang, Y.; Hu, H.; Chen, G. *Chem. Mater.* **2008**, *20*, 1670.
(42) Li, C. L.; Wang, Y. Q.; Shi, B. F.; Ren, J. W.; Liu, X. H.; Wang, Y. G.; Guo, Y.; Guo, Y. L.; Lu, G. Z. *Microporous Mesoporous Mater.* **2009**, *117*, 104.
(43) Holland, B. T. *Microporous Mesoporous Mater.* **2006**, *89*, 291–299.
(44) Petushkov, A.; Merilis, G.; Larsen, S. C. *Microporous Mesoporous Mater.* **2011**, *143*, 97.
(45) Mintova, S.; Valtchev, V.; Onfroy, T.; Marichal, C.; Knoezinger, H.; Bein, T. *Microporous Mesoporous Mater.* **2006**, *90*, 237.
(46) Camblor, M. A.; Corma, A.; Valencia, S. *Microporous Mesoporous Mater.* **1998**, *25*, 59.
(47) Tosheva, L.; Valtchev, V. P. *Chem. Mater.* **2005**, *17*, 2494.
(48) Van Oers, C. J.; Stevens, W. J. J.; Bruijn, E.; Mertens, M.; Lebedev, O. I.; Van Tendeloo, G.; Meynen, V.; Cool, P. *Microporous Mesoporous Mater.* **2009**, *120*, 29.
(49) Hould, N. D.; Kumar, S.; Tsapatsis, M.; Nikolakis, V.; Lobo, R. F. *Langmuir* **2010**, *26*, 1260.
(50) Möller, K.; Yilmaz, B.; Müller, U.; Bein, T. *J. Am. Chem. Soc.* **2011**, *133*, 5284.